

Sensorized Foam Actuator with Intrinsic Proprioception and Tunable Stiffness Behavior for Soft Robots

Saravana Prashanth Murali Babu*¹, Francesco Visentin¹, Ali Sadeghi¹, Alessio Mondini¹, Fabian Meder¹, and Barbara Mazzolai*¹

¹Affiliation not available

March 15, 2021

Abstract

This Supporting information includes:

1. Component Selection and Performance of SFA
2. Actuator Manufacturing and Preparation of Conductive Ink
3. Average Thickness of Conductive Coating layer on PU Foam
4. Time Response of the Actuator in Different Modes
5. Characterization and Experimental Setup
6. Measurement and Data Analysis
7. Design Specifications of Soft Robotic Applications
8. Supporting Video

Corresponding author Email: saravanaprashanth@outlook.com, barbara.mazzolai@iit.it

1. Component Selection and Performance of SFA

Components	Company/Material
Materials and devices	
Copper plate adhesive	3M 1245 Tape
Silver epoxy	Chemtronics, CW2400
Support frame	Delrin or POM
Foam	Modulor, GmbH, 033035
Fiber-reinforced skin	3M, Scotch 1900
Paper sheets	Cellulose fibers
Wire	Insulated copper wire
Pneumatic connector	Silicone and PP (polypropylene)
Laser cutter	Versalaser ULS 3.0
Foam cutter	Custom-made (wire-cut)
Electronics and Mechanical components	
Controller	Custom-made
Electro-valves	Parker, X-valve
Voltage divider circuit	Custom-made
Data acquisition system	NI USB 6219
Oil lubricated rotary vane pump	MM56p2, D.V.P Vacuum Technology s.r.l
Pneumatic pump (approx. +50 kPa to -50 kPa)	Parker, Micro diaphragm pump

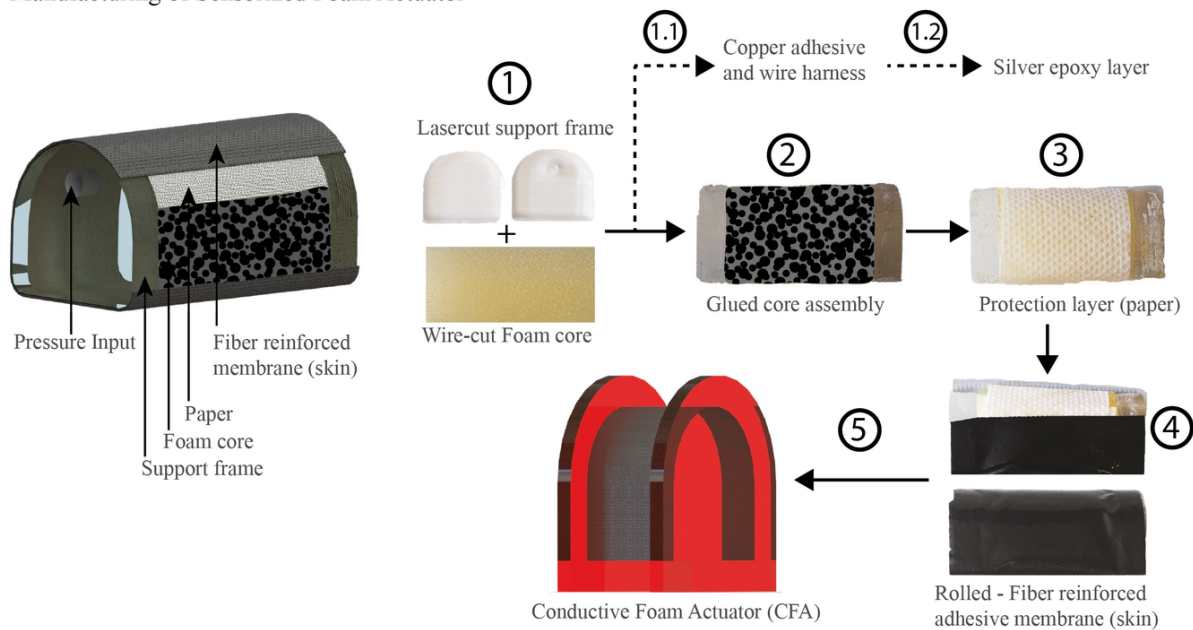
Table 1: Required components needed to build the integrated SFA.

Component (parameters)	Value	Unit
Area		
Form core	2168.7	mm ³
Module weight		
Assembled SFA	34	g
Actuation		
Positive pressure (P_p)	[10 - 40]	kPa
Negative pressure (N_p)	[10 - 90]	kPa
Actuation period		
Active compression	4000	ms
Relaxation time (T_r)		
Mode 1 (only N_p)	5.35	s
Mode 2 (both N_p and P_p)	1.5	s
Relative resistance ($\Delta R/R_O$)		
Passive compression (skin)	64	%
Active (vacuum)	95	%
Maximum force (F_{max})	235 @ -90	N @ kPa

Table 2: Performance and Physical Parameters of the SFA.

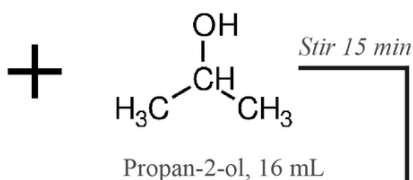
2. Actuator Manufacturing and Preparation of Conductive Ink

A) Manufacturing of Sensorized Foam Actuator

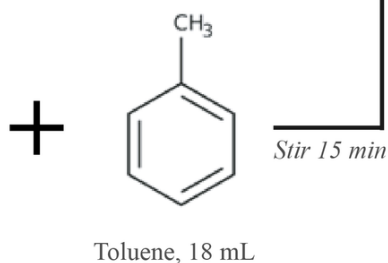


B) Preparation of conductive ink

Step 1



Step 2



5 times Dipped and squeezed

Conductive Foam

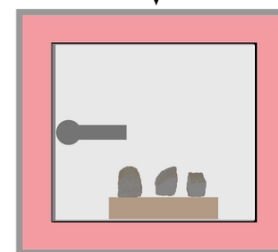


Figure 1: A) Manufacturing steps involving easy-to-do laser cut of the support structures and wire-cut conductive foam for batch manufacturing process. Glued core assembly comes with support frame sandwiched with copper plate (Advanced Leicester) and a layer of silver epoxy (Chemtronics). Later part is then encapsulated with a layer of paper and fiber reinforced adhesive skin. The same procedures are followed for different size and shape of the actuator. Final step is to connect the one end of the actuator to the pressure

3. Average Thickness on Conductive Coating Layer on PU

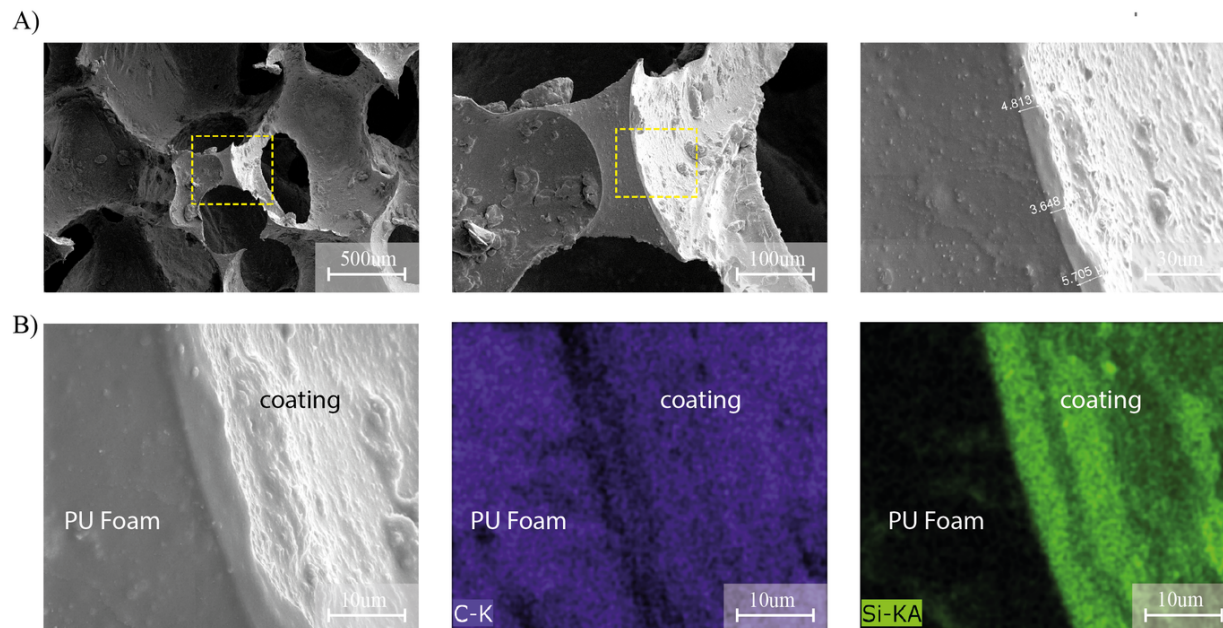


Figure 2: A) Scanning electron microscopy (SEM) image of the coated conductive foam. Samples were prepared by sectioning the conductive foam and observation in the SEM without further sputtering showing an average thickness of the coating layer of $\sim 4.29 \pm 0.5 \mu\text{m}$ over the PU foam. B) Microanalysis of the conductive foam was performed clearly showing carbon 'C' in coating and PU foam whereas silicon 'Si' is only present in the coating due to the silicone elastomer in the conductive ink.

4. Time Response of the Actuator in Different Modes

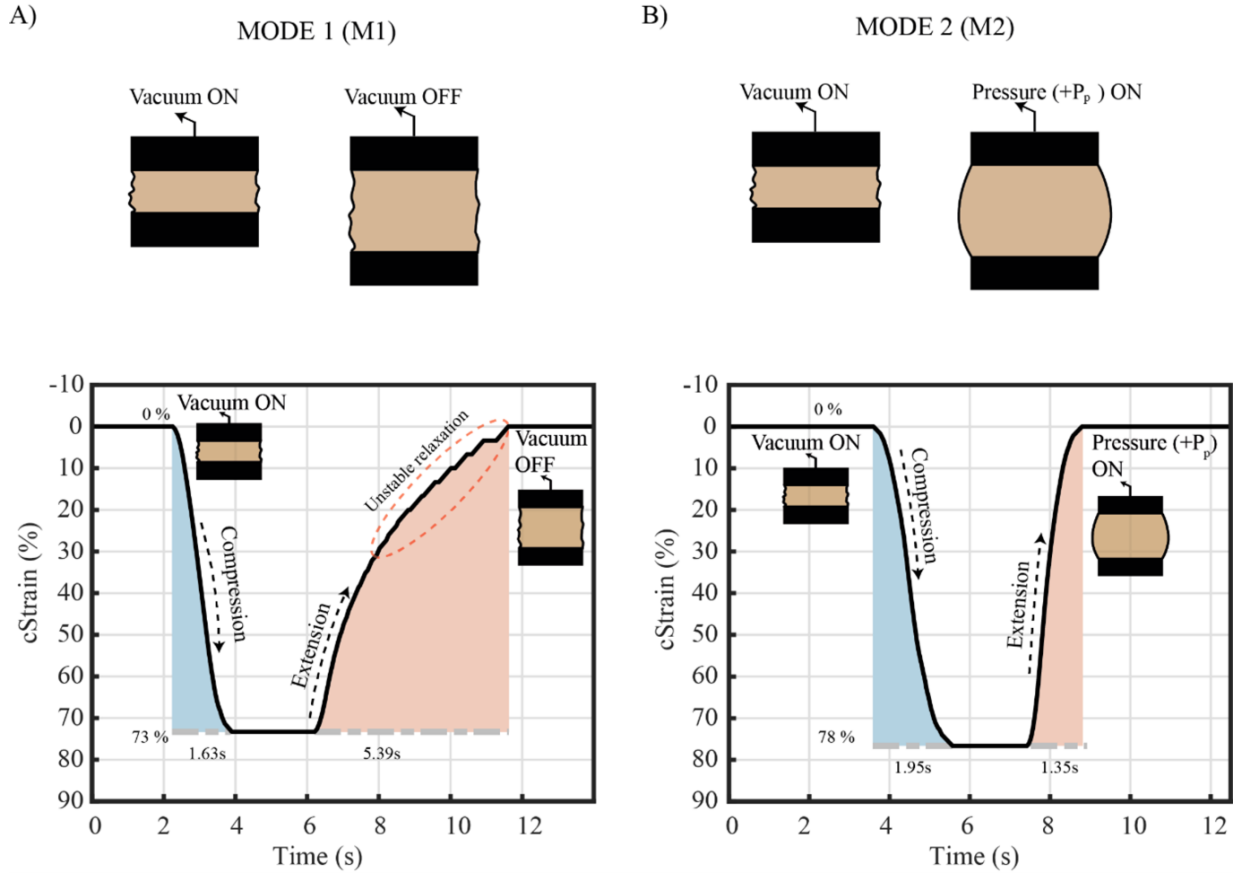


Figure 3: Response of the SFA to the various active actuation modes. A) Mode 1 actuation (vacuum @ -90 kPa followed by passive decompression) showing a slower response during relaxation phase with some unstable zones while recovering. B) Mode 2 actuation (vacuum @ -90 kPa followed by active decompression using 10 kPa) showing a response that is five times faster and more stable. Plots are an average over 20 cycles. Mode 2 is faster and more accurate than mode 1 which is five times slower with some instability during the relaxation phase.

5. Characterization and Experimental Setup

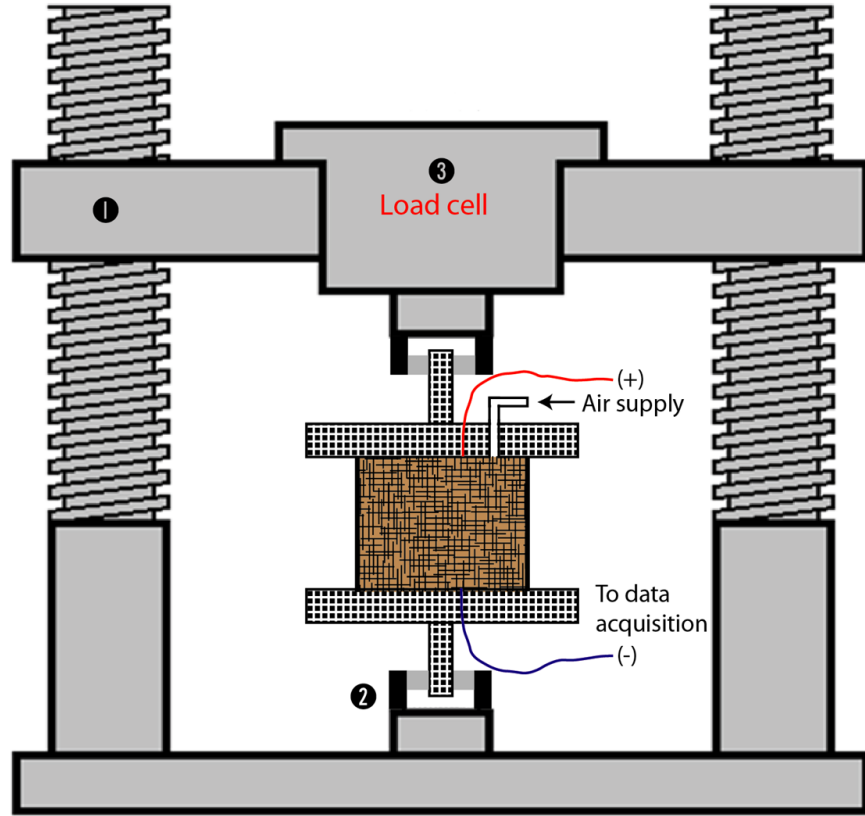


Figure 4: Illustrative setup of static measurement device (zwick/roell, Z005) used for characterization experiments. 1) Movable linear stage used to compress the actuator module in a constant speed of 30 mm/min without any additional disturbance. 2) Mechanical pressurized clamps with gripper in order to hold the actuator modules in place preventing from mechanical instability. 3) Load cell of 1 kN from Zwick and Roell to measure the extension or pulling force of the actuator under different circumstances such as variable pressure, different size and mode of actuation. The sequence of experimental procedure are as follows, first the pressure input is turned on (actuated) which pulls the actuator along with the loadcell causing increase in the force and the linear stages compresses down to 20 mm displacement and then pulled up to the original state. This is repeated for 11 cycles for every characterization experiments.

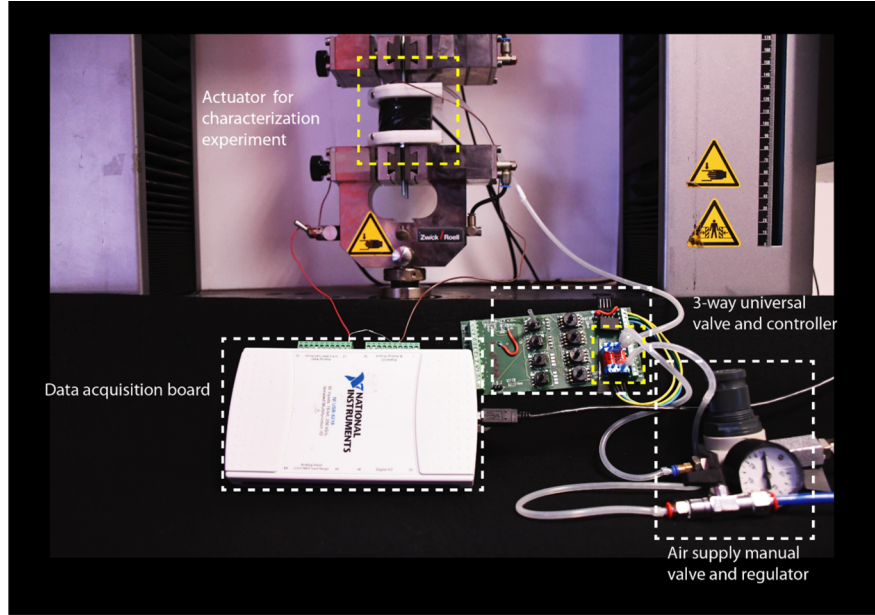


Figure 5: Instrumentation setup for SFA experiments. NI USB 6229 DAQ used for data acquisition of change in voltage from the actuator to the voltage divider circuit, later post processed to visualize relative resistance. Air supply channel for both positive and negative pressure with manual valve and regulator. 3-way universal electro valves (yellow dotted lines) are used to control the input pressure using the controller board which actuates the actuator based on the driven square wave signal sequence from the computer. Characterization and experimental setup are described in figure S4.

6. Measurement and Data Analysis

Porosity calculation:

By considering the sample of total volume as V_t . Defining the solid phase to be of volume V_s , and the volume of the pore phase (the holes) to be V_p , with $V_t = V_s + V_p$. The volume fraction of the pore phase or porosity is denoted by $\phi = V_p/V_t$. The solid volume fraction is then $1 - \phi$.^[1]

By assuming these values, (assumptions were made from the average pore size and that of the solid modelling analysis)

Volume in solid phase (V_s) is 24102.88 mm^3

Volume in pore phase (V_p) is 16068.5 mm^3

Using the above defined information, the porosity is calculated to be $\phi = 0.66$

Passive actuation mode:

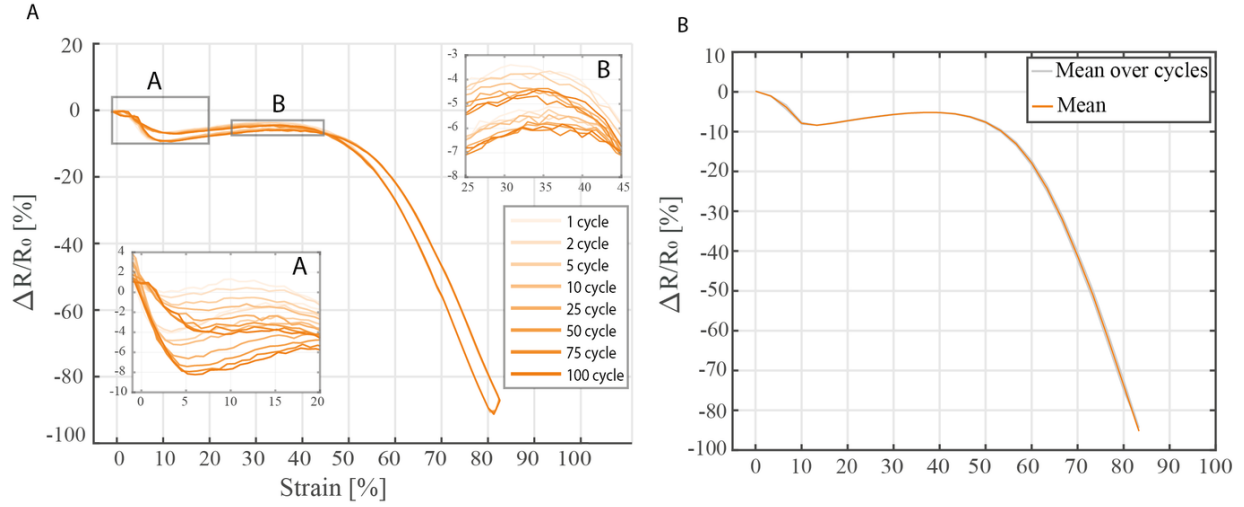


Figure 6: A) Resistance change at selected cycles (1 - 100). The zoomed-in box 'A' show a large drift in the sensor data in a strain interval of 0 % to 20 %. The zoomed-in box 'B' show a small drift in sensor data in a strain profile of 25 % to 45 %. B) Hysteresis of the actuator during passive actuation mode and the mean over cycles with a small drift error of 6%.

Active actuation mode:

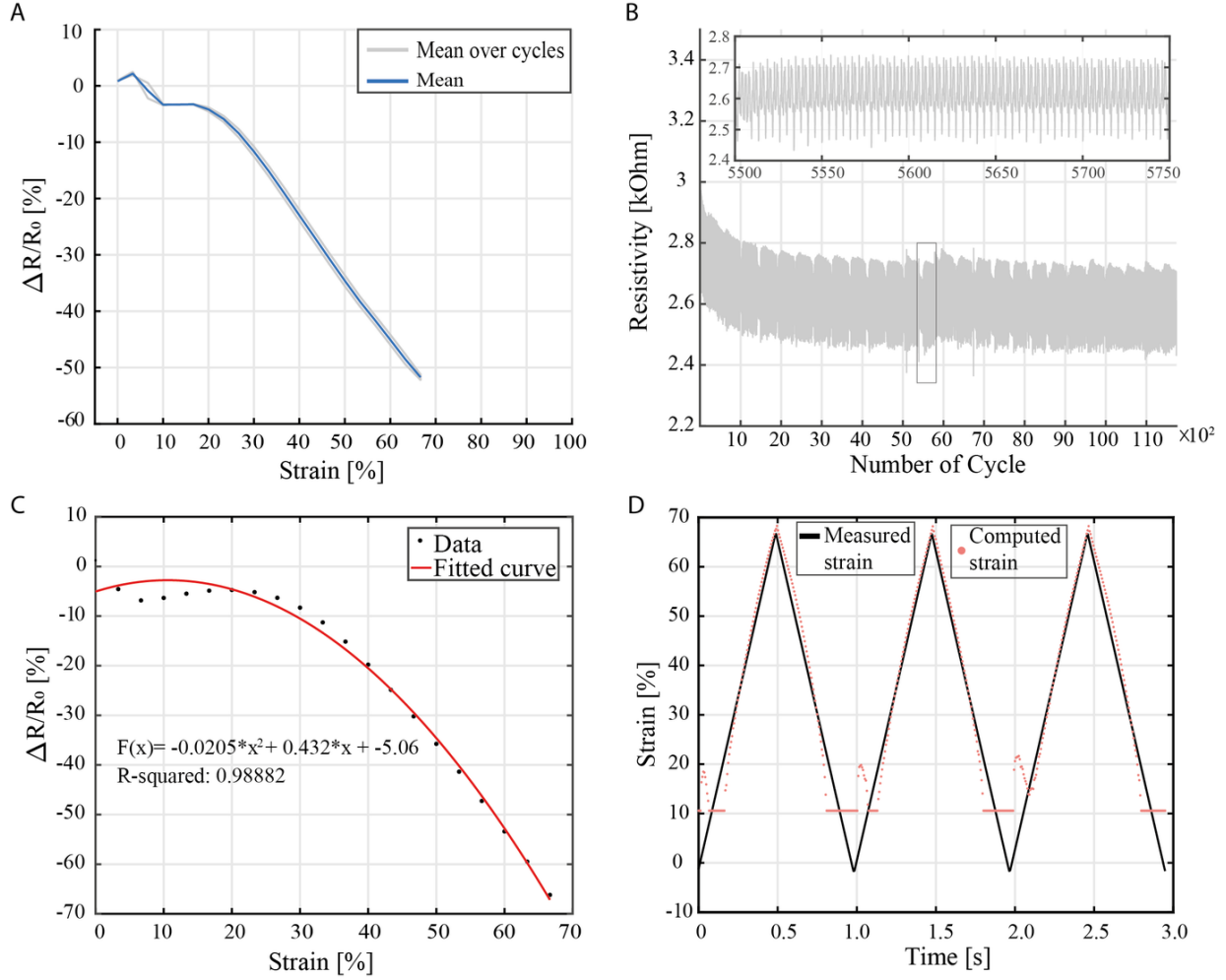


Figure 7: A) Hysteresis of the actuator during passive actuation mode and the mean over cycles with a small drift error of less than 4 %. B) Cyclic test for more than 10000 to confirm the robustness and reliability of the sensorized foam. C) Fitting curve of the relative resistance data with the given function showing an accuracy value of R^2 equal to 0.988. D) Evaluation of the accuracy of the fitting used to retrieve the strain from the changes in the relative resistivity. As it is possible to notice, the data show a linear relationship (error < 15%) for strain larger than 22% while for lower compression value the data deviate from the fitting with larger errors (40%). The relationship between the real and the computed strain value is plotted in **Figure 2E**.

Displacement (mm)	Strain (%)	Force @ -30 kPa (N)	Force @ -60 kPa (N)	Force @ -90 kPa (N)
0	0	0	0	0
5	17	24	31.5	92
10	34	33	48	150
15	50	42	61	190
20	70	68	88	230

Table 3: Force value for the active compression case under variable pressure inputs with displacement interval of very 5mm up to 20mm.

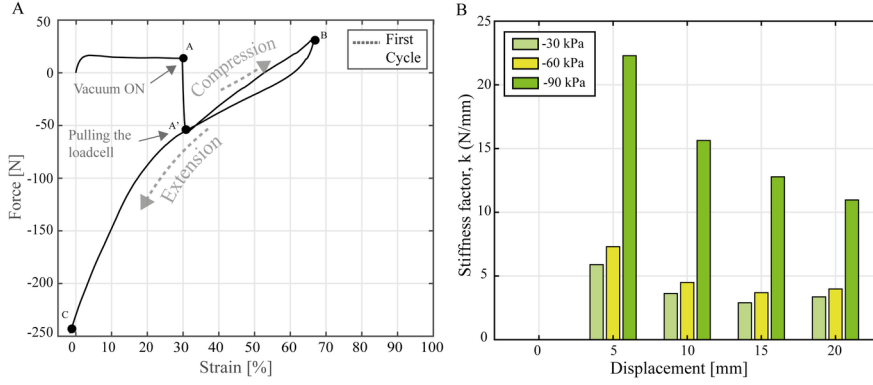


Figure 8: A) Force reading with the initial response of the actuator before applied vacuum (A) and after applied vacuum (A') and from here it compresses down to 70% of the strain upto point B and pulled back to the initial position (c). Thereafter goes with the cyclic compression and extension phase of the actuator. This is to support the result shown in **Figure 3A**. B) Tunable stiffness of the actuator at multiple pressure input (-30, -60, -90) kPa exhibiting increase in stiffness factor (k) during extension profile of the sensorized actuator. This is to support the result shown in **Figure 3D** and the corresponding value of 'k' stiffness factor is shown in the table below **Table S3**.

Displacement (mm)	Strain (%)	k @ -30 kPa (N/mm)	k @ -60 kPa (N/mm)	k @ -90 kPa (N/mm)
0	0	0	0	0
5	17	5.9	7.3	22.3
10	34	3.6	4.5	15.6
15	50	3	3.7	12.8
20	70	3.3	4	11

Table 4: Stiffness value for the active compression case under variable pressure inputs with displacement interval of very 5mm up to 20mm.

7. Design Specifications of Soft Robotic Applications

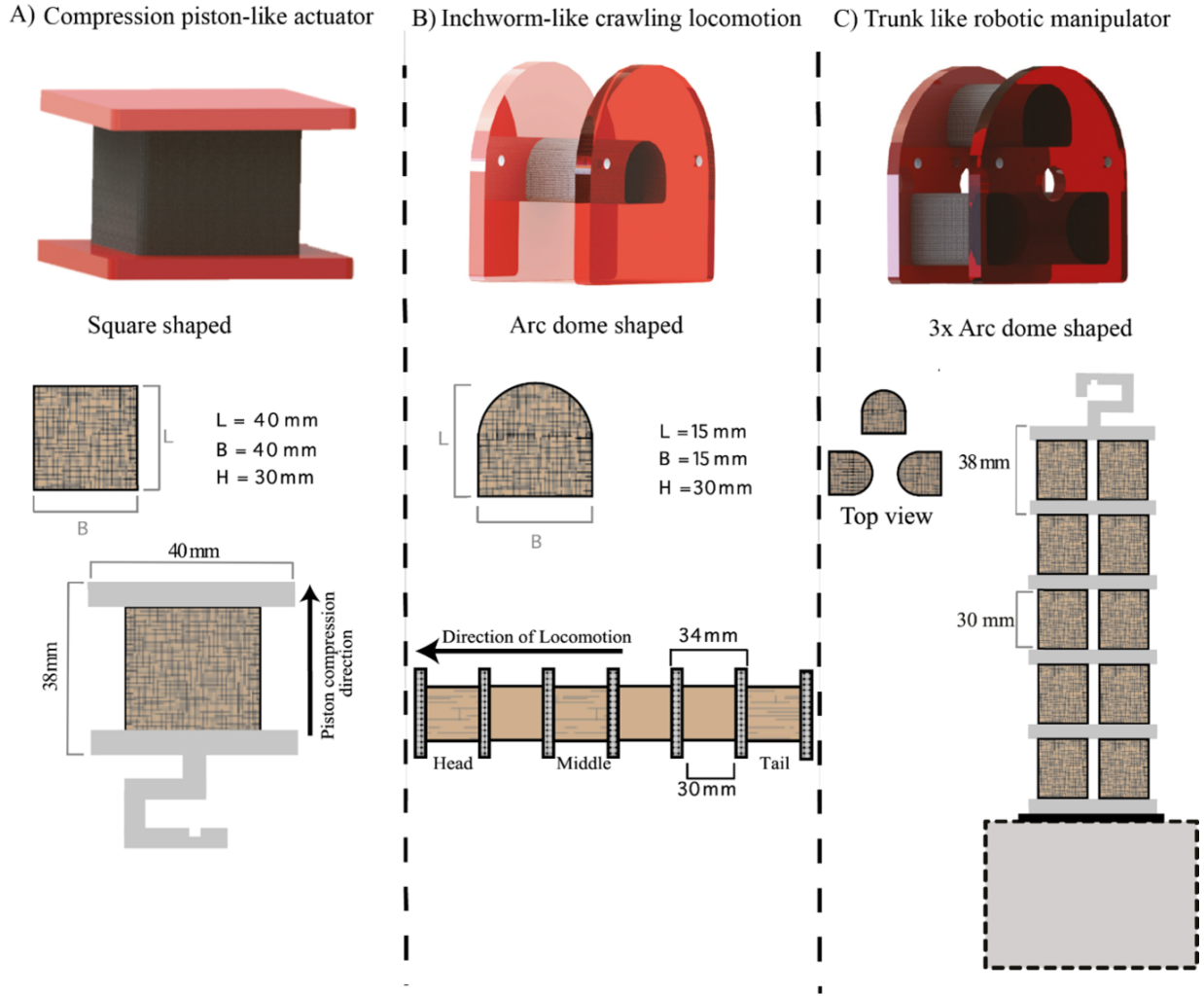


Figure 9: Illustrative description and details of the robot built using SFA's and their details. A) compression piston-like actuator built using the design of square shaped large sized actuator. The hanger in the bottom was printed using SLA 3D printer (Formlab 2, Formlabs inc.) in order to place a hanger and step increase in the load from no load up to 6 kg. B) crawling locomotion robot was built using the design of arc dome shaped small sized actuator. Each of the them are connected in series to forms a modular structure for inchworm-like crawling locomotion. 1st, 3rd and 6th are the one measuring the relative resistance during every gait cycle. C) Trunk-like robotic manipulator was built in a different configuration by arranging three arc dome-shaped small sized actuators adjacent to one another at an angle 90° parallel and perpendicular to each other. This configuration helps the module to rotate, compress and extend the actuator. From the top 1st, and 4th were the one marked for measuring the change detected during manipulating under load and no load condition.

8. Supporting Video

Rich media available at <https://youtu.be/Po7L3XCLS9k>

Rich media available at <https://youtu.be/1zDKgZGjjFk>

Rich media available at <https://youtu.be/4mre2MZGsT0>

Rich media available at <https://youtu.be/3L1SMwj5Xcs>

Rich media available at <https://youtu.be/INxoPvHgiZ0>

Rich media available at <https://youtu.be/U99UW04szEA>

Rich media available at https://youtu.be/AlT_U22d3aI

Rich media available at <https://youtu.be/QiJCaeQ4EaQ>

References

- [1] E. J. Garboczi, D. P. Bentz, N. S. Martys, *Methods in the Physics of Porous Media* **1999**, 35, 1.